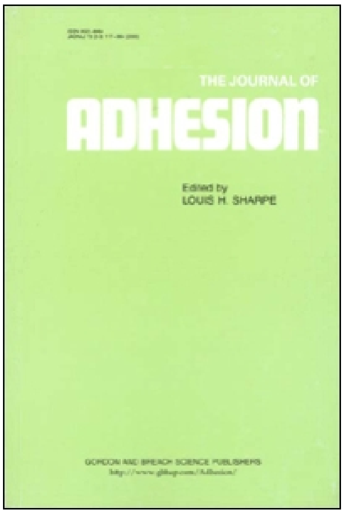

The Journal of Adhesion
Publication details, including instructions for authors and subscription information:
http://www.informaworld.com/smpp/title~content=t713453635

The Effects of Cure Temperature and Time on the Stress-Whitening Behavior of Structural Adhesives. Part I. Analysis of Bulk Tensile Data

Hooshang Jozavi[a]; Erol Sancaktar[a]
[a] Department of Mechanical and Industrial Engineering, Clarkson University, Potsdam, New York, U.S.A.

To cite this Article Jozavi, Hooshang and Sancaktar, Erol(1989) 'The Effects of Cure Temperature and Time on the Stress-Whitening Behavior of Structural Adhesives. Part I. Analysis of Bulk Tensile Data', The Journal of Adhesion, 27: 3, 143 — 157
To link to this Article: DOI: 10.1080/00218468908048449
URL: http://dx.doi.org/10.1080/00218468908048449

J. Adhesion, 1989, Vol. 27, pp. 143–157
Reprints available directly from the publisher
Photocopying permitted by license only

Printed in the United Kingdom

The Effects of Cure Temperature and Time on the Stress-Whitening Behavior of Structural Adhesives. Part I. Analysis of Bulk Tensile Data

HOOSHANG JOZAVI and EROL SANCAKTAR

Department of Mechanical and Industrial Engineering, Clarkson University, Potsdam, New York 13676, U.S.A.

(Received November 21, 1987; in final form September 9, 1988)

The phenomenon of stress whitening in rubber-modified thermosetting polymers has been observed and reported by several researchers. It is necessary to define and characterize the stress-whitening stress σ^* and strain ε^* values for modified structural adhesives since they define localized material failure more accurately (in comparison with the tensile strength) from a fracture point of view. Such characterization should include variation with respect to cure parameters since they are known to affect bulk tensile properties. For this purpose, an analytical method of defining and calculating the σ^* and ε^* values is reviewed. The analytical method consists of a modified bilinear form of the Ramberg–Osgood equation which is used in conjunction with bulk tensile data.

As a novel approach, the inverses of the Ramberg–Osgood exponents n_1 and n_2 are related to material strength and failure behaviors as a function of cure temperature. The stress-whitening stress levels are also related to the cure temperature. It is shown that the variations of $1/n_1$ and $1/n_2$ with respect to the cure temperature are similar to the variations of the tensile strength (σ_y) and the fracture toughness (K_{IC}) respectively.

KEY WORDS Stress-whitening stress and strain; bilinear Ramberg-Osgood equation; effects of cure temperature, time and cool down rate; crack tip plastic deformation zone; adhesive fracture; adhesive constitutive behavior.

INTRODUCTION

During our current investigations with Metlbond 1113 and 1113-2 rubber-toughened epoxy adhesives (with and without carrier cloth, respectively) it was observed that stress whitening takes place prior to complete failure. This observation was made with bulk tensile[1] and shear,[2] and bulk[3] and bonded[4] fracture samples. On the microscopic scale, stress whitening is caused by cavitation, voiding and rupture of the rubbery phase due to the high triaxial stress state which exists at the dispersed rubber particles and in close proximity to them. This local failure process is followed by coalescence of the formed cavities through shear banding and usually results in gross failure. Stress whitening is an energy-dissipative mechanism due to the creation of new surfaces during the cavitation process. For this reason, the phase separation and/or dispersion of the rubbery phase, which can be monitored in the cure process, will serve to toughen the brittle epoxy matrix. It should be noted that even though cavitation occurs as a result of a triaxial state of stress on a microscopic scale, the global bulk stress-whitening stress σ^* value, corresponding to the occurrence of local failure events in the specimen, is defined and measured as a macroscopic uniaxial stress on a bulk specimen.

During our investigations the extent of stress whitening observed on the surfaces of bulk tensile and fracture specimens varied with cure conditions and, consequently, the degree of cure. Higher cure temperatures tended to increase the extent of stress whitening while low cure temperatures reduced it.

Yee *et al.*[5,6] conducted mechanical and microscopy studies on the toughening mechanisms in rubber-modified epoxies. They performed microscopic investigations on the bulk tensile and three-point bend (TPB) Single Edge Notched (SEN) specimens in order to study the nature of stress whitening of a number of epoxies with varying degrees of rubber content. They found that, in the absence of rubber, no stress whitening was observed during the deformation and fracture of their model epoxy resins. They also found that as the rubber content is increased, the size of the crack tip whitening as well as fracture energy (G_{IC}) increases. Through Scanning Electron Microscopy (SEM) of the whitened zone, they found that rubber particles and the matrix had cavitated and that the size of these cavities was larger than the diameters of the undeformed rubber particles as determined by TEM. They also reported that the stress-whitening effect visible to the naked eye is simply due to the scattering of light from these cavitated regions. They maintained that the energy dissipation, crack tip blunting capability and/or toughening mechanisms of these materials are facilitated through fracture of rubber phase at the walls of the cavities in stress-whitened zones.

Kinloch[7] reports that one of the most successful methods of increasing the toughness of thermosetting adhesives is to incorporate a second phase of dispersed rubbery particles into the cross-linked polymer. He states that the cure conditions have a profound effect on the microstructure of rubber-toughened epoxies and that the cure time-temperature curve marking the end of phase separation decreases with decreasing cure temperature and increasing logarithm of cure time. This curve lies slightly above the similarly-behaving gelation curve for the epoxy phase. Vitrification of the epoxy phase is stated to occur beyond the end of phase separation of the rubber particles. Kinloch[7] also states that the deformation processes which dissipate energy in the vicinity of a crack tip in rubber-toughened epoxies are: i) cavitation in the rubber, or at the rubber/matrix interface, and ii) plastic shear yielding localized in the bulk of the epoxy matrix. Kinloch[7] concludes that it is this localized cavitation process that gives rise to the stress whitening which often accompanies crack growth.

O'Connor,[8] in his investigations on the adhesive fracture energy (G_{IC}) of

Metlbond 1113-2 (in bonded form) observed a stress-whitened zone preceding the tip of the propagating crack. He found that the length of this zone remained ~0.53 in. (13.5 mm) during crack propagation.

In elastoplastic analysis of brittle epoxy adhesives several investigators[4,9,10] used Irwin's[11] concept of a plastic deformation zone at the tip of a crack to resolve the issue of stress singularity at that location. The approximate diameter for this zone, calculated on the basis of measured Mode I strain energy release rate G_{IC} and bulk tensile properties (tensile strength, Young's modulus and, Poisson's ratio), was also suggested as the optimum adhesive thickness for bonded joints.[4,9] This suggestion was offered to ensure obtaining the maximum G_{IC} value in bonded specimens as it is obtained in bulk samples.

As confirmed by visual and microscopic evidence, it is the authors' belief that such a plastic deformation zone at the tip of a crack encompasses the stress-whitened zone. An exact corrolation between the plastic zone diameter and the size and shape of the stress-whitened zone is not yet available. Since Irwin's analysis is based on a small scale yielding assumption and does not describe the shape of the plastic deformation zone accurately, the presence of a circular deformation zone should be considered only hypothetical. In fact, mathematical functions describing the exact shape of crack tip plastic deformation zones are available in the literature for monolithic samples.[12,13]

Without going into the discussion of the exact shape for the stress whitened zone, we will present a methodology and data on stress whitening which, we hope, will serve as the first step in analyzing its exact distribution. For this purpose two sequential papers will be presented. The first paper will discuss the use of bulk tensile data in defining and measuring the stress-whitening stress as a material property. The authors would like to emphasize that the mechanical behavior of the model adhesives, as well as similar structural adhesives, are affected by the rate of straining. The constant strain rate stress-strain behavior of these adhesives approaches a perfectly elastic-plastic behavior as the magnitude of strain rate is increased. In other words, especially at higher strain rates, the yield stress σ_y increases and approaches to the value of the ultimate stress σ_{ult}. Thus, in adopting the Linear Elastic Fracture Mechanics (LEFM) methodology, we will define the σ_y as the ultimate tensile strength or as the failure stress. One of the major goals of this paper is to show that it may be more appropriate to use the stress-whitening stress σ^* instead of σ_y, due to the stress whitening observed just prior to rupture. The use of σ^* as the local failure stress in specific boundary value problems involving stress concentration, such as the crack tip stress state, is proposed, because the occurrence of the whitened zone represents localized cavitated zones, microcracks and shear bands which, upon further increase in loading, coalesce, propagate and cause gross failure.

The second paper will concentrate on fractographic data. In both papers the effects of important parameters, such as cure temperature, time and cool-down rate, on the stress-whitening phenomenon will also be presented.

The bulk tensile properties and behavior of Metlbond 1113 and 1113-2 model adhesives subjected to constant-head-rate tensile loading were investigated by Brinson *et al.*[14,15] They investigated the time and rate-dependent behavior of the model adhesives and proposed several models that could fit the stress-strain behavior. They found that the most suitable model that would fit the stress-strain response of the model adhesives, with prediction of the stress-whitening stress level (σ^*), was a modified version of Ramberg–Osgood equation[16] which they called the "Bilinear RAMOD-2" equation. The bilinear behavior was obtained when log ε_p was plotted against log σ. The plastic strain ε_p was assumed to be a function of the over-stress above the elastic-limit stress, and the stress levels defining the intersection point for the bilinear behavior were found to occur slightly below the stress-whitening stress (σ^*) values.

Brinson *et al.*[14,15] reported that the adhesive material properties were different before and after stress-whitening due to changes in material behavior and therefore bilinear equations were needed to describe such behavior. Specifically, they determined that the Poisson's ratio decreased considerably once the stress-whitening had occurred. This reduction was as much as 42% when the Poisson's ratio decreased from 0.388 to 0.266. They also reported that the σ^* increased with increasing initial elastic strain rate. It should also be noted that the largest difference beween the σ^* and σ_y reported by Brinson *et al.*[14,15] was 2.7%. They also performed loading-unloading experiments on the model adhesives. Beyond the elastic limit stress, unloading resulted in higher levels of plastic strains as the initial loading stresses were increased.

Obviously, σ^* is an important material property for the bulk adhesive because it is the parameter that truly defines localized material failure from a fracture point of view. For example, the authors think that in elastoplastic fracture mechanics calculations using σ^* in calculating K_{IC} may be more appropriate than using σ_y. In light of this consideration it becomes necessary to optimize σ^* as a function of cure temperature and time. For this purpose, data obtained by bulk tensile testing of Metlbond 1113 adhesive is utilized in this paper. Metlbond 1113 is a 100% solids, modified nitrile-epoxy film with a synthetic carrier cloth, and it is commercially available from Narmco Materials Inc. (Costa Mesa, California, U.S.A.) in 0.25 mm-thick, solid film rolls. The bulk tensile stress-strain data are fitted with the bilinear RAMOD-2 model and, consequently, the σ^* and the exponents n_1 and n_2 of the Ramberg–Osgood equations are determined. As a novel approach, the inverses of the exponents n_1 and n_2 are related to material strength and failure behaviors as a function of cure temperature. The stress-whitening stress levels are also related to the cure temperature and time conditions.

In Part II of this paper, fracture data obtained using SEN tension specimens of the same model adhesive will be studied in relation to stress whitening at the crack tip. For this purpose, scanning electron photomicrographs will be utilized and the effects of cure temperature and time on the stress-whitening behavior at the crack tip will be investigated. A brief discussion on the formation and effects of inherent voids will also be presented in Part II since they are observed to enhance the crack tip whitening zones.

ANALYTICAL CONSIDERATIONS

It is appropriate to introduce some background on the Ramberg–Osgood (RAMOD) equation and the bilinear RAMOD-2 model. Assuming that plastic strains are functions of the current state of stress and independent of the loading history, Kachanov[17] proposed the following stress-strain relation:

$$\varepsilon_{ij} = (\sigma_{mm}/9K)\,\delta_{ij} + \psi S_{ij} \tag{1}$$

where $K = E/3(1-v)$ is the bulk modulus. The term ψ is a scalar function of the invariants of the stress tensor as indicated by Hill.[18] The terms ε_{ij}, σ_{ij}, δ_{ij} and S_{ij} represent the strain, stress, the Kronecker Delta and deviatoric stress tensors respectively. For the case of uniaxial tension Eq. (1) reduces to

$$\varepsilon = \sigma/E + \phi\sigma \tag{2}$$

where the subscripts have been dropped and $\phi = 2/3\psi$ is often determined empirically to fit the experimental data. Following the same assumptions, the Ramberg–Osgood equation,[15] which was originally proposed for the uniaxial tensile and compressive behavior of various metal alloys, is given as

$$\varepsilon = \sigma/E + K\sigma^n \tag{3}$$

where K and n are material constants and E is the elastic modulus. It is evident that Eq. (3) is a special form of Eq. (2) where $\phi = K\sigma^{n-1}$ is taken as a function of σ. Note that the terms on the right hand side of Eq. (3) represent the elastic (ε_e) and plastic (ε_p) strains respectively. Therefore, one may be able to approximate values of K and n from a log-log linear plot of σ *versus* ε_p.

After a number of modifications to Eq. (3), Renieri *et al.*[15] determined that a bilinear form of Eq.(3) in which the plastic strain would be a function of the overstress, *i.e.* $(\sigma - \theta)$ where θ is the elastic limit stress, could successfully be fitted with experimental data up to failure. Thus, the bilinear RAMOD-2 has the form:

$$\begin{aligned} &\varepsilon = \sigma/E && 0 \le \sigma \le \theta \\ &\varepsilon = \sigma/E + K_1(\sigma - \theta)^{n_1} && \theta \le \sigma \le \sigma^* \\ &\varepsilon = \sigma/E + K_2(\sigma - \theta)^{n_2} && \sigma^* \le \sigma \le \sigma_{\max} \end{aligned} \tag{4}$$

where K_1, n_1, K_2 and n_2 are the material constants determined empirically from a bilinear log–log plot of ε_p *versus* $(\sigma - \theta)$. In the bilinear RAMOD-2 model, σ^* is defined as the stress at the intersection of the bilinear plots of log ε_p *versus* $\log(\sigma - \theta)$.

Renieri *et al.*[15] observed that Eq. (4) could best fit their stress-strain-rate results for Metlbond 1113 and 1113-2. Moreover, they realized the significance of σ^* and its variation with strain rate in connection with the stress-whitening phenomenon that occurred in the tensile samples before fracture. They observed the stress-whitening stress and strain values experimentally (through visual observation). They found that σ^* and the corresponding strain values (ε^*) as determined from Eq. (4) were very close to the experimentally-observed values at stress whitening. Therefore, one may hypothesize that the presence of stress whitening and existence of σ^*, *i.e.* a bend in the log ε_p *vs.* $\log(\sigma - \theta)$ data, are directly related. It should be mentioned that in Reference 15 the experimentally-observed stress-whitening stresses and strains were slightly higher than those determined through the bilinear RAMOD-2 model, because the experimental observations were made by the naked eye. Thus, the actual stress-whitening stress and strain values may have even been closer to the empirically-determined σ^* and ε^* values.

In this paper, the physical significance of the bilinear RAMOD-2 model with respect to variation in the cure conditions is considered. Equation (4) indicates that the inverse of n_1 and n_2, *i.e.* $1/n_1$ and $1/n_2$, may be related to the different softening behaviors prior to and after the stress whitening. In other words, a higher $1/n_1$ would indicate higher extent of cure, less shrinkage stresses, less degradation, less softening and, consequently, more stable material behavior prior to stress whitening. We believe, therefore, that the material behavior represented by the parameter $1/n_1$ is similar to what is represented by the tensile strength (σ_y) of the bulk material. Moreover, $1/n_2$ may be related to the softening after stress whitening up to failure. Therefore, higher $1/n_2$ values would indicate higher resistance to complete failure and resistance to propagation of microcracks that eventually result in total failure.

In elastoplastic fracture mechanics it is frequently assumed that the failure stress at the crack tip is equal to the uniaxial yield stress acting over a region called the plastic zone. For Mode I loading, Irwin[11] approximated the diameter of this plastic deformation zone to be

$$r_p = K_{IC}^2/\pi\sigma_y^2, \tag{5}$$

The authors propose that the use of σ^* rather than σ_y in Eq. (5) may be more appropriate even though the numerical difference between σ^* and σ_y for some structural adhesives is not very large (2.7% maximum for Metlbond). The reason for this proposal is the fact that σ^* represents local failure in the bulk material more closely than σ_y does. Furthermore, the material behavior after σ^* has been reached (locally), as represented the parameter $1/n_2$, is of great importance in relating local failures to catastrophic failures in flawed structures. The authors think that the material behavior represented by the parameter $1/n_2$ is similar to what is represented by the fracture toughness (K_{IC}) of the bulk material.

EXPERIMENTAL PROCEDURES

Details of the preparation and testing of bulk tensile and fracture specimens have previously been reported.[1,3]

Cure Schedules for Bulk Tensile Specimens

The following abbreviated notation is used to specify the material, cure time, cure temperature and cool-down as $M_{i,j,c}$ where

M: material; A for Metlbond 1113

i: cure time (minutes) and $i = 1, \ldots, 9$, see Table I,

j: cure temperature and $j = 1, \ldots,$ see Table I,

c: cool-down condition; "f" for fast, and "s" for slow cool-down condition.

The following example illustrate the use of this convention:

A2, 5, f: Metlbond 1113 sample cured for 20 minutes at 93°C and subjected to a fast cool-down condition.

The cure time and temperature schedules originally proposed for bulk tensile (constant head rate) and fracture testing[1,3] contained a large spectrum as shown in Table I. However, a number of them were eliminated or not reported either i) due to incomplete cure and hence inability to handle or ii) because there were other conditions already tested which would yield a trend for a property of interest. Samples (bulk tensile) from the latter category were for cure times of 30,200 and 500 minutes.

The manufacturer's recommended cure schedules for the Metlbond 1113 adhesive in the bonded form were the (2, 10) (3, 9) and (4, 5) schedules (see Table I) which are referred to as 'fast', 'standard' and 'low' respectively. Moreover, the manufacturer suggests a vented pressure of 103-345 kPa during cure.

It should also be mentioned here that the failure sections of the bulk tensile samples were observed to contain varying amounts of voids for different cure

TABLE I
Cure schedules and notations

Cure time (Min.)	Index i	Cure temperature °F(°C)	Index j
10	1	115(46)	1
20	2	140(60)	2
30	3	170(77)	3
120	4	185(85)	4
200	5	200(93)	5
500	6	215(102)	6
1,000	7	230(110)	7
5,000	8	245(118)	8
10,000	9	260(127)	9
		290(143)	10
		320(160)	11
		350(177)	12
		380(193)	13

conditions. As an approximate method of determining the effective load-bearing sections, the total void areas were measured, using optical microscopy, and subtracted from the nominal cross sections to correct the nominal engineering stress values.

For this purpose, it was assumed that the failure section of the bulk tensile samples contained the largest void area and that the measured sizes of the voids did not change during the loading process. Hence, if the void ratio is denoted as the ratio of voided area (A_v) to the nominal section area (A_T) then the engineering stress may be modified by using the active area $(1 - A_v/A_T)$ ratio. Therefore, the corrected stress ($\sigma_{corr.}$) is calculated as:

$$\sigma_{corr.} = \sigma/(1 - A_v/A_T) \tag{6}$$

where σ is the engineering stress based on the initial section area (A_T).

The effect of this correction procedure on the adhesive tensile stress and stress whitening stress *vs.* cure temperature curves can be seen in Figures 5 and 6 respectively. Further information on void formation will be presented in Part II of this paper.

RESULTS AND DISCUSSION

The bilinear RAMOD-2 model was applied to the stress-strain behavior of Metlbond 1113 adhesive cured under different schedules. The elastic limit stress (θ) and strain (ε_0) values were obtained from the experimental engineering stress-strain data.[1] The $\varepsilon_p = \varepsilon - \varepsilon_0$ *versus* $\sigma - \theta$ values were plotted on log–log scales and the parameters of the bilinear RAMOD-2 model, *i.e.* K_1, n_1, K_2 and n_2, were determined by using simple linear regression of these data. When they existed, the locations of σ^* and ε^* were determined as the intersection of the two linear portions in the log ε_p *vs.* $\log(\sigma - \theta)$ plots. It was found that the bilinear RAMOD-2 could be fitted to the experimental data very closely (with a correlation coefficient of greater than 0.999) even up to failure.

An important observation regarding the existence of σ^* (in the bilinear RAMOD-2) and the presence of stress whitening was made when this model was used in conjunction with Metlbond 1113 data. For the specimens that did not exhibit any stress whitening prior to failure, *i.e.* for those with very low cure temperatures or very short cure times, no σ^* could be clearly detected. In other words, for these cases the log ε_p *vs.* $\log(\sigma - \theta)$ plots were straight lines (with correlation coefficients of $\sim$1) up to failure without any bend (*i.e.* σ^* did not exist).

The bilinear RAMOD-2 model parameters, *i.e.* n_1, K_1, n_2, K_2, σ^* and ε^*, as determined for Metlbond 1113 with different cure conditions, are listed in Table II. The parameters corresponding to the cases with no σ^*, and hence no stress whitening observation, have not been included in this table.

Figure 1 shows the application of the bilinear RAMOD-2 model to the stress-strain-cure temperature behavior of Metlbond 1113 specimens subjected to

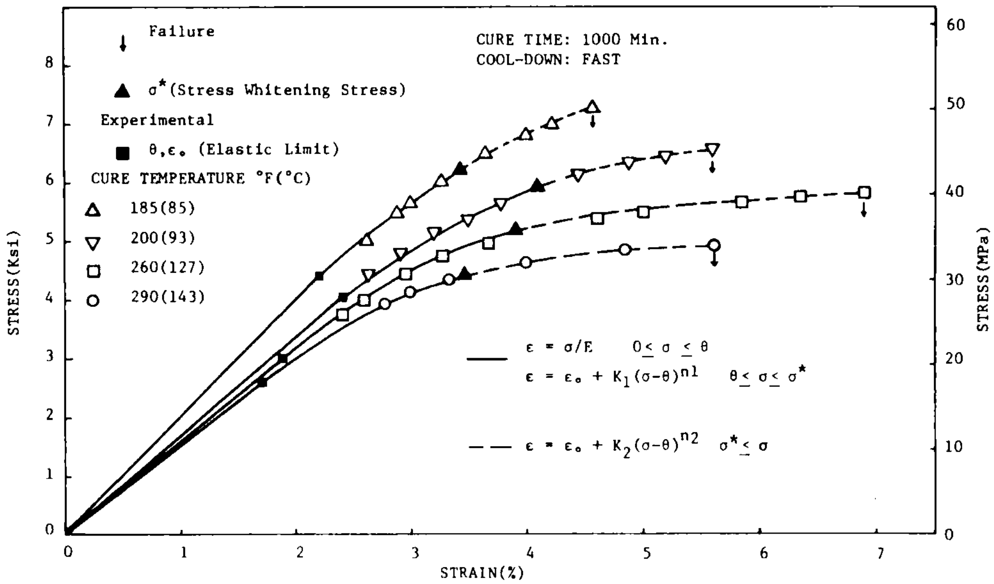

FIGURE 1 The effects of cure history on the tensile stress-strain behavior of Metlbond 1113 and comparison with the bilinear RAMOD-2 model.

1000-min. cure and fast cool-down conditions. It can be seen that excellent agreement exists between the experimental results and theoretical prediction even up to failure. Moreover, the existence of σ^* and stress whitening (observed for all cases shown in Figure 1) provides additional information revealing the effects of cure temperature on the bulk tensile stress-strain behavior of Metlbond 1113. Figure 1 also reveals the similarity in variations of elastic limit stress, σ^* and tensile strength values with respect to cure temperature. The variation of ε^* (stress-whitening strain) with cure, however, is observed to be similar to that of the elastic limit strain (ε_0) rather than the maximum failure strain (ε_{max}). Figure 2 shows the application of the bilinear RAMOD-2 model to the 10000-min. cured samples of Metlbond 1113. As mentioned earlier, no σ^* could be detected for the 46°C cure temperature specimens as no stress whitening was observed. Again, the agreement between the experimental results and the bilinear RAMOD-2 model prediction seems to be very satisfactory.

Figure 3 shows the variation of $1/n_1$ and $1/n_2$ parameters for Metlbond 1113 with cure temperatures as averaged over all cure times. The variation of the parameter $1/n_2$ with cure temperature is somewhat similar to the variation of the fracture toughness K_{IC} for the same material (Figure 4). The variation of $1/n_1$, however, clearly indicates the existence of a peak at the 104°C cure temperature below and above which smaller values are obtained. The cure temperature corresponding to the peak $1/n_1$ value (Figure 3) and the peak for the optimum strength-cure curve (corrected for the presence of void areas on the failure section of the specimens), shown in Figure 5, can be correlated with the

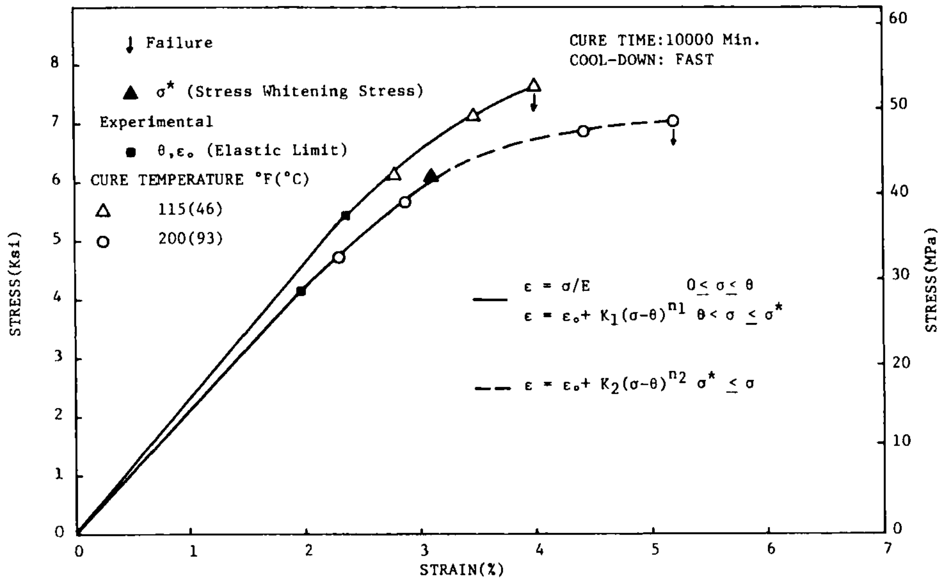

FIGURE 2 The effects of cure history on the tensile stress-strain behavior of Metlbond 1113 and comparison with the bilinear RAMOD-2 model.

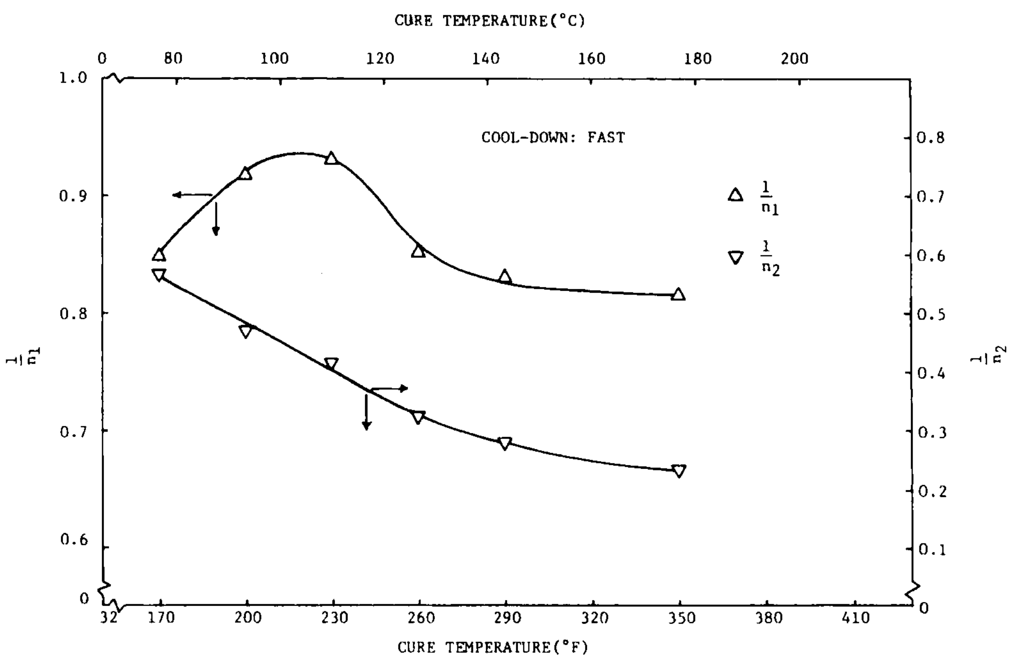

FIGURE 3 The effects of cure temperature on the inverse exponents of the bilinear RAMOD-2 model predicted from the stress-strain behavior of Metlbond 1113 (averaged for all cure times).

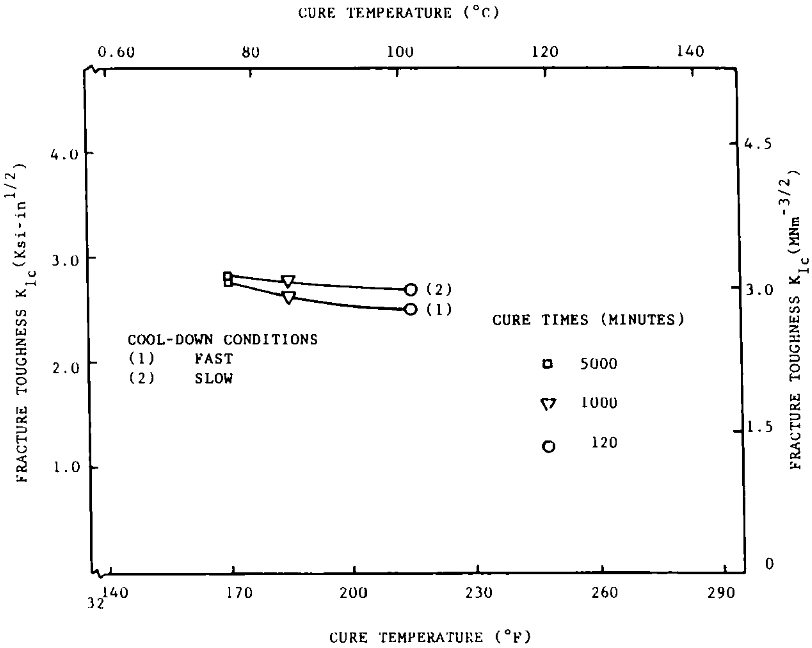

FIGURE 4 Comparison of Metlbond 1113 fracture toughness-cure optimization curves for the slow and fast cool-down conditions.

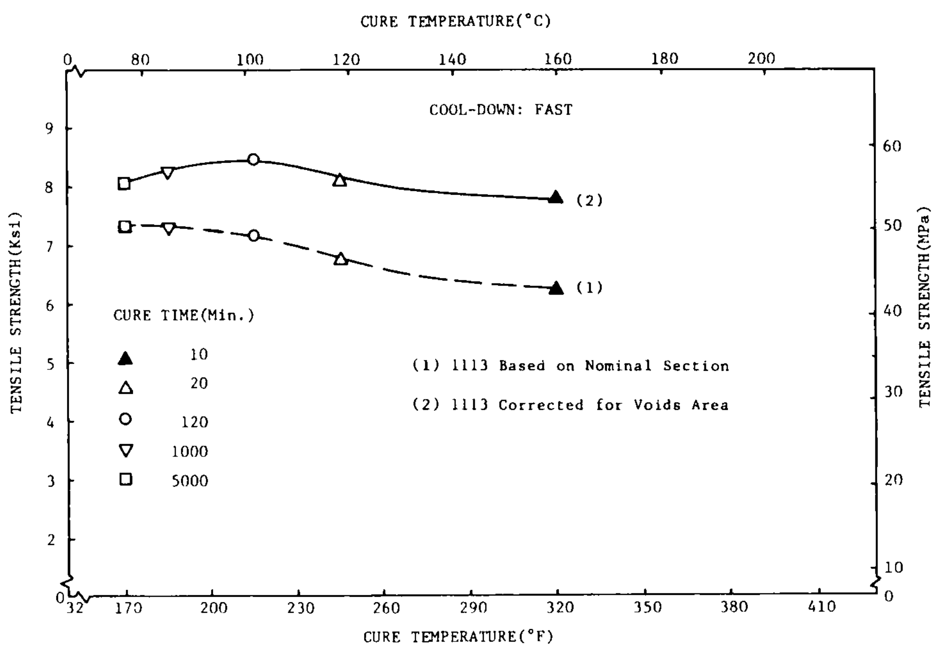

FIGURE 5 Metlbond 1113 optimum strength-cure behavior (with and without void area correction).

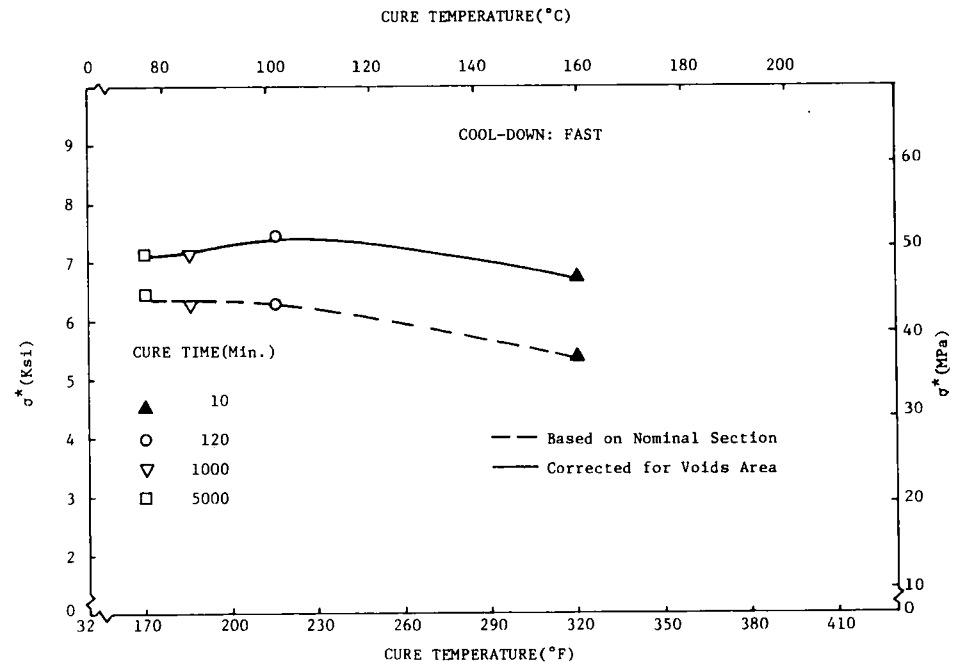

FIGURE 6 Variation of σ^* (stress whitening stress) based on the bilinear RAMOD-2 model for Metlbond 1113 corresponding to the cure conditions giving optimum strength.

maximum glass transition temperature ($Tg \sim 112°C$) detected for Metlbond 1113.[19] It seems that for sufficient cure times (*e.g.* 120 minutes) the optimum cure temperature for Metlbond 1113 would lie somewhere between 99°C and 110°C, in order to obtain the best strength performance of the model adhesive.

The σ^* values corresponding to the optimized strength-cure data for Metlbond 1113 subjected to the fast cool-down condition are shown in Figure 6, with and without void area correction. It may be observed that the void area correction affects the variation of σ^* for optimum cure conditions by indicating a slight peak around the 102°C cure temperature in a fashion similar to that of tensile strength. (Figure 5). In other words, with void correction the optimum cure temperature is now at 102°C and it coincides well with the maximum glass transition temperature. Further discussion on the formation and effects of inherent voids will be presented in Part II of this paper.

It should also be noted that σ^*, $1/n_1$ and the tensile strength (σ_y) all exhibit similar behavior with respect to cure temperature. Furthermore, the peak (optimum) values for all three parameters lie somewhere between 99°C and 110°C in good correlation with the T_g (~112°C) of the model adhesive. These findings confirm our initial assertion that the material behavior represented by $1/n_1$ is similar to what is represented by the tensile strength of the bulk adhesive.

The effects of cool-down conditions on the RAMOD-2 parameters are shown in Table II. Examination of Table II reveals that higher σ^* values are obtained

TABLE II
Parameters of the bilinear RAMOD-2 model

Sample	n_1	K_1 (psi$^{-n_1}$)	n_2	K_2 (psi$^{-n_2}$)	σ^* (MPa)	ε^* (%)
A1, 11, f	1.00	6.95E − 6	2.68	2.77E − 11	36.98	2.93
A1, 12, f	1.23	1.70E − 6	4.26	2.27E − 16	39.82	3.64
A1, 13, f	1.05	4.70E − 6	7.64	5.00E − 28	40.93	3.40
A2, 7, f	1.04	6.22E − 6	2.13	2.18E − 09	37.05	4.02
A2, 9, f	1.29	1.08E − 6	3.68	1.50E − 14	36.86	3.80
A2, 10, f	1.26	1.26E − 6	3.76	8.00E − 15	33.42	3.33
A3, 7, f	1.06	5.60E − 6	2.34	2.50E − 10	35.14	3.52
A3, 9, f	1.05	7.00E − 6	2.72	5.00E − 11	33.62	3.58
A3, 10, f	1.20	2.08E − 6	3.19	8.40E − 13	30.18	3.15
A4, 5, f	1.10	2.99E − 6	2.06	2.28E − 09	42.37	3.36
A4, 6, f	0.99	7.30E − 6	1.93	5.79E − 09	43.40	3.46
A4, 7, f	1.06	5.26E − 6	1.96	5.89E − 09	38.24	3.60
A4, 9, f	1.15	2.60E − 6	3.00	2.27E − 12	36.52	3.42
A4, 10, f	1.07	5.06E − 6	3.91	3.20E − 15	33.42	3.02
A7, 3, f	1.12	2.89E − 6	1.82	1.51E − 08	41.34	3.43
A7, 4, f	0.99	6.46E − 6	1.65	4.54E − 08	43.04	3.42
A7, 5, f	1.21	1.86E − 6	2.05	3.25E − 09	40.88	4.10
A7, 7, f	1.25	1.39E − 6	2.76	1.60E − 11	36.17	3.82
A7, 9, f	1.24	1.51E − 6	3.15	7.06E − 13	36.11	3.87
A7, 10, f	1.31	9.41E − 7	4.23	2.61E − 16	30.82	3.45
A8, 3, f	1.24	9.70E − 7	1.71	2.65E − 08	44.56	3.39
A8, 5, f	1.05	4.40E − 6	2.45	9.30E − 11	43.75	3.24
A8, 7, f	1.01	6.35E − 6	2.47	9.49E − 11	38.93	3.10
A8, 10, f	1.36	5.50E − 7	3.10	1.28E − 12	36.17	3.06
A9, 5, f	1.02	5.22E − 6	2.32	2.84E − 08	41.96	3.11
A1, 11, s	1.04	5.70E − 6	2.16	4.95E − 11	43.82	3.87
A2, 5, s	1.13	2.86E − 6	2.38	1.57E − 10	40.86	3.80
A2, 7, s	0.85	1.80E − 5	1.98	4.37E − 09	42.03	3.90
A2, 9, s	0.91	1.16E − 5	2.04	2.37E − 09	39.75	3.06
A2, 10, s	0.99	9.60E − 6	2.97	4.45E − 12	37.20	3.92
A3, 5, s	1.19	1.37E − 6	1.26	7.80E − 07	31.69	1.88
A3, 10, s	1.12	3.10E − 6	2.59	4.60E − 11	33.76	3.25
A4, 5, s	1.03	4.20E − 6	2.16	6.90E − 10	37.55	2.52
A4, 10, s	1.20	1.58E − 6	3.86	2.40E − 15	39.14	3.39
A7, 4, s	1.07	3.80E − 6	1.61	6.80E − 08	46.85	3.53
A7, 5, s	1.15	1.74E − 6	2.42	9.03E − 11	42.72	3.10
A7, 10, s	1.18	1.50E − 6	2.76	5.87E − 12	40.10	3.26
A8, 3, s	1.10	2.60E − 6	2.43	7.93E − 11	50.30	3.55

when slow cool-down conditions are used. The slow cool down condition also results in higher $1/n_1$ and $1/n_2$ values, in general.

SUMMARY AND CONCLUSIONS

It was pointed out that rubber-toughened epoxy adhesives exhibit stress whitening in bulk or bonded specimens prior to complete failure. The plastic deformation zone at the crack tip of an adhesive sample encompasses the stress-whitened zone. Consequently, it is necessary to define and characterize the stress-whitening stress σ^* and strain ε^* values because they define localized material failure more accurately from a fracture point of view. Such characterization should include variation with respect to cure parameters since they are known to affect bulk tensile properties. For this purpose, an analytical method of defining and calculating the σ^* and ε^* values was reviewed. The analytical method consisted of a modified bilinear form of the Ramberg–Osgood equation (RAMOD-2) which was used in conjunction with bulk tensile data.

As a novel approach, the inverses of the Ramberg-Osgood exponents n_1 and n_2 were related to material strength and failure behaviors as a function of cure temperature. The stress-whitening stress levels were also related to the cure temperature and time conditions.

It was asserted that higher $1/n_1$ values indicate higher σ values. The higher $1/n_2$ values, on the other hand, indicate higher resistance to complete failure and resistance to propagation of microcracks that eventually result in total failure. Both of these assertions were confirmed experimentally, since the variations of $1/n_1$ and $1/n_2$ with respect to the cure temperature were shown to be similar to the variations of σ_y and K_{IC}, respectively.

The experimental results revealed that RAMOD-2 model could be fitted to the experimental data very closely.

The cure conditions: temperature, time and cool-down rate were shown to affect, considerably, the Ramberg-Osgood exponent n_1 and the stress-whitening parameters σ^* and $1/n_2$. The stress-whitening stress (σ^*), the inverse Ramberg-Osgood exponent ($1/n_1$), and the tensile strength (σ_y) all exhibited similar behavior with respect to cure temperature with peaks in the 99°C to 110°C range, which coincides well with the T_g for the model adhesive. The slow cool-down condition resulted in higher σ^*, $1/n_1$ and $1/n_2$ values which indicated higher resistance to fracture (Table II).

The material behavior represented by the parameter $1/n_2$ was shown to be somewhat similar to what is represented by the fracture toughness (K_{IC}) of the adhesive material. Both $1/n_2$ and K_{IC} exhibited a decreasing behavior when the cure temperature was increased.

Fractographic data revealing the effects of cure temperature and time on the crack tip stress-whitening behavior of the same model adhesive and further discussion on formation and effects of inherent voids will be presented in Part II of this paper.

Acknowledgements

This work was partially supported by the National Science Foundation under Grant No. GME-8007251.

References

1. E. Sancaktar, H. Jozavi and R. M. Klein, *J. Adhesion* **15**, 241 (1983).
2. E. Sancaktar, *Experimenal Techniques* **8**, 27 (1984).
3. H. Jozavi and E. Sancaktar, *J. Adhesion* **18**, 25 (1985).

4. E. Sancaktar, H. Jozavi and J. Baldwin, *Proceedings of the Southeastern XIIIth Conference on Theoretical and Applied Mechanics* **2,** 752 (1986).
5. A. F. Yee and R. A. Pearson, *J. Maths. Science* **21,** 2462 (1986).
6. R. A. Pearson and A. F. Yee, *ibid* **21,** 2475 (1986).
7. A. J. Kinloch, Abstracts, Eighth Annual Meeting of The Adhesion Society, 6a (1985).
8. D. G. O'Connor, *Factors Affecting the Fracture Energy for a Structural Adhesive,* Master's Thesis, Virginia Polytechnic Institute and State University, August 1979.
9. W. D. Bascom, R. L. Cottington and C. D. Timmons, *J. Appl. Polym. Sci.* **32,** 165 (1977).
10. D. L. Hunston, A. J. Kinloch, S. J. Shaw and S. S. Wang, in *Adhesive Joints,* K. L. Mittal, Ed. (Plenum Press, New York, 1984), pp. 789–807.
11. G. R. Irwin, *Proc. 7th Sagamore Conf.,* IV (1960), pp. 63–173.
12. D. Broek, *Elementary Engineering Fracture Mechanics,* 3rd Ed. (Noordhoff International Publishing, Leyden, Netherlands, 1974).
13. J. W. Dally and R. J. Sanford, *Proceedings of the 1985 SEM Spring Conference on Experimental Mechanics,* pp. 851–860.
14. H. F. Brinson, M. P. Renieri and C. T. Herakovich, ASTM STP 593 (Am. Soc. for Testing and Matls., Philadelphia, 1975), pp. 177–199.
15. M. P. Renieri, C. T. Herakovich and H. F. Brinson, *Rate and Time Dependent Behavior of Structural Adhesives,* Virginia Polytechnic Institute Report No. VPI-E-76-7 April 1976.
16. W. Ramberg and W. R. Osgood, *Description of Stress-Strain Curves by Three Parameters,* NACA TN 902, April 1943.
17. L. M. Kachanov, *Foundations of the Theory of Plasticity* (North Holland Publishing Co., Amsterdam, 1971).
18. R. Hill, *The Mathematical Theory of Plasticity* (Oxford University Press, London, 1956).
19. H. Jozavi, *The Effects of Cure Temperature and Time on the Bulk Tensile and Fracture Behavior of a Structural Adhesive.* Ph.D. Dissertation, Clarkson University, March 1987.